



## On reaction pathways in the conversion of methanol to hydrocarbons on HZSM-5



Xianyong Sun, Sebastian Mueller, Yue Liu, Hui Shi, Gary L. Haller, Maricruz Sanchez-Sanchez, Andre C. van Veen<sup>1</sup>, Johannes A. Lercher\*

Department of Chemistry and Catalysis Research Center, Technische Universität München, Lichtenbergstrasse 4, D-85747 Garching, Germany

### ARTICLE INFO

#### Article history:

Received 16 April 2014

Revised 13 June 2014

Accepted 14 June 2014

#### Keywords:

Methanol to olefins

ZSM-5

Hydrocarbon pool

Mechanism

### ABSTRACT

The underlying mechanisms of the two distinct catalytic cycles operating during conversion of methanol to olefins (MTO) on HZSM-5 have been elucidated under industrially relevant conditions. The co-existence of olefins and aromatic molecules in the zeolite pores leads to competition between the two cycles. Therefore, their importance depends on the local chemical potential of specific carbon species and the methanol conversion. Due to a faster, “autocatalytic” reaction pathway in the olefin based cycle, olefin homologation/cracking is dominant under MTO conditions, irrespective of whether aromatic molecules or olefins are co-fed with methanol. Another hydrogen transfer pathway, faster than the usual route, has been identified, which is directly linked to methanol. In agreement with that, the co-feeding of olefins resulted in a remarkable longer lifetime of the catalyst under MTO conditions, because the high rate methylation competes with the formation of more deactivating coke – presumably oxygenates– through methanol derivatives.

© 2014 Elsevier Inc. All rights reserved.

### 1. Introduction

The catalytic conversion of methanol to olefins (MTO) has drawn particular attention in recent years, as this process is believed to provide an alternative pathway for the production of ethene and propene [1–4]. One of the key issues of the MTO chemistry, the control of product selectivity, necessitates a fundamental understanding of the reaction mechanism. The extremely complex reaction network makes this, however, a very challenging task [5–7].

The initial debate was mainly focused on how the first C–C bond was formed. Over 20 direct coupling mechanisms were suggested in spite of little experimental evidence [2,8,9]. Recent experimental and theoretical investigations suggested, however, that direct C–C coupling is not the dominating pathway due to unstable intermediates and prohibitively high activation barriers [8–10]. Several mechanisms involving impurities in the feedstock appear to offer more plausible reaction routes for the formation of initial hydrocarbons.

In 1979, Chen and Reagan originally proposed that MTH is an autocatalytic reaction [11]. Consistent with this proposal, an olefin homologation/cracking route was suggested by Dessau and

co-workers as the main reaction pathway on HZSM-5 at steady-state conditions [12,13]. After the initial olefins are formed during the induction period, these olefins are consecutively methylated to form higher olefin homologues, which in turn crack into lighter olefins such as ethene and propene. Hydrogen transfer and cyclization reactions lead to the formation of alkanes and aromatics as end products. In parallel with the proposal of this olefin based cycle, the important role of aromatics and unsaturated cyclic species in the methanol reaction has also been proposed. Langner et al. for example reported that co-feeding 36 ppm of cyclohexanol significantly reduced the duration of the induction period [14]. In a parallel study, experiments of co-feeding toluene or *p*-xylene with methanol led Mole et al. to postulate a co-catalytic effect of methylbenzenes on methanol conversion [15,16]. As the conversion of methanol produces aromatic molecules, one could also identify the aromatics based reaction routes as another form of autocatalysis. These early investigations were very insightful and embodied already the concept of aromatics based cycle. However, these findings remained largely ignored.

It was the invention of SAPO-34 material in the 80s that stimulated again the investigations in the early 1990s of the role of aromatics in the MTH reaction and subsequently the proposal of the “hydrocarbon pool” concept by Kolboe et al. [17–19]. In the original proposal, the active center was a “coke-like” organic species adsorbed on the surface [17–19]. The active site for MTO was later defined as a supramolecular inorganic–organic hybrid (zeolite-

\* Corresponding author. Fax: +49 8928913544.

E-mail address: [johannes.lercher@ch.tum.de](mailto:johannes.lercher@ch.tum.de) (J.A. Lercher).

<sup>1</sup> Present address: The University of Warwick, School of Engineering, Library Road, Coventry CV4 7AL, United Kingdom.

hydrocarbon species), which acts as a scaffold for light olefin formation [20,7]. The unique structure of SAPO-34 material provided the possibility of trapping carbon intermediate species and, thus, stimulated intensive investigations in parallel by groups of Kolboe and Haw, respectively. This established the role of aromatics, especially polymethylbenzenes and their protonated forms, as the active hydrocarbon pool species in SAPO-34, H-BEA, and H-MOR catalysts have large pores or cages [20,7,21–30]. Recent experimental and theoretical work proposed that olefins may act as another kind of active hydrocarbon pool species, particularly in medium-pore zeolites, such as the ZSM-22 zeolite with 1-D 10-ring channels, in which the internal spaces are too small to form polymethylbenzenes [31–34].

In retrospect, the MTO history clearly demonstrated that the actual course of the mechanistic understanding developed in loops, and the key mechanistic aspects that are generally accepted today were reported already in the very early literature [5]. Both, the olefin-based cycle and the aromatic-based route are well accepted at present by researchers favoring either the early “autocatalysis” proposal or the later “hydrocarbon pool” concept [5,6]. However, further insights into the dynamic course of the interactions of zeolite (acid sites), hydrocarbon species, and methanol are yet to be developed, some of which we try to address in the present work.

Although a general rationale of the zeolite-specific product distribution has been achieved through understanding the kinetic consequences of the zeolite topology and the identity of the active hydrocarbon species, for zeolites such as H-BEA, SAPO-34 or HZSM-5, where probably both catalytic cycles work, a quantitative relationship between these cycles and the product distribution has not been unequivocally established [5,6]. For instance, although several reports have shown that aromatics, especially higher polymethylbenzenes, are active hydrocarbon pool species in H-BEA zeolite at 623 K [29,30], recent investigations by Ahn et al. and Simonetti et al. [35,36] demonstrated that, over H-BEA, the olefin based cycle can be selectively favored over the aromatics based cycle, and the carbenium-ion chemistry dictates the formation of a product pool rich in highly branched C<sub>4</sub> and C<sub>7</sub> alkanes by using low temperatures (473 K) and moderate DME partial pressures (>50 kPa). Therefore, the reaction conditions, in addition to zeolite topology, play a remarkable role in involvement of the active hydrocarbon species and the product selectivity.

The same situation applies to HZSM-5. The archetypical catalyst for methanol conversion to gasoline – and in recent years light olefins – has attracted tremendous efforts to elucidate the mechanism (e.g. [1–2,5–6]). A more recent study of the group of Olsbye summarized the proposals for a dual-cycle mechanism on HZSM-5 [5]. An aromatics-based cycle involved ethene and methylbenzenes, and the olefin-based methylation/cracking cycle produces C<sub>3+</sub> olefins [37,38]. This has been a seminal contribution to the interpretation of HZSM-5 specific product distributions. However, compared to the typically chosen temperatures (≤623 K) for these mechanistic studies, higher reaction temperatures (≥723 K) are used in the case of HZSM-5 based industrial processes [5], such as the Air Liquide’s MTP process, for which a recycling operation of the aliphatic products other than propene is incorporated [39–42]. As a result, tailoring product distributions requires insight into the reaction mechanism under realistic reaction conditions and specific operation modes.

Thus, we report here the elucidation of the kinetic aspects of the mechanism under reaction conditions closely related to the practical operations, i.e., the intrinsic selectivities toward ethene and propene formation of the aromatics- or olefins-based cycles, and how the dominant reaction pathways are influenced by feed composition, how they change during the reaction course, and, ultimately, how each cycle contributes to methanol conversion and the specific product distributions.

## 2. Experimental

The employed catalyst and other reagents are identical with the materials used in the previous paper [43]. The zeolite powder has a Si/Al ratio of 90 and crystal size of 500 nm. The catalytic tests were performed on either a bench-scale plug flow reaction unit (with nitrogen dilution) or 10-fold parallel reaction unit (using water as diluent). The pressed, crushed, and then fractionized zeolite pellets are diluted, loaded and processed with the identical procedures as reported in Ref. [43].

In the experiment addressing the MTO reaction cycles, a fixed catalyst amount of 20 mg was loaded into the reactor. The methanol partial pressure in the flow is held constant at 10 kPa by maintaining the temperature of methanol saturator at 299 K. The total flow rate was systematically changed to achieve different space velocities. After the reaction temperature was stabilized under 50 ml/min N<sub>2</sub> flow at 723 K for 1 h, the N<sub>2</sub> flow was passed through the methanol saturator to achieve 10 kPa methanol. After 5 min on stream, the GC was started to measure the reactor effluent composition, and subsequently the valve for the feed control was switched to pure N<sub>2</sub> flow and the N<sub>2</sub> flow rate was set to the target value. This procedure was repeated for a series of space velocities.

The experiments for the aromatics co-feeding were conducted as previously described [43]. The methanol partial pressure was 10 kPa, while the *para*-xylene partial pressure was 0.2 kPa, both diluted by N<sub>2</sub>. The total flow rate was maintained, as the catalyst charged was changed to reach different levels of conversions. In the experiments for the conversion of pure olefins (120 C%), i.e., 1-pentene, 1-hexene or 1-heptene, experiments were performed under reaction conditions as close as possible to those applied in the MTO reaction of a feed containing 10 kPa methanol (100 C%) and 0.4 kPa 1-pentene (20 C%). 10 kPa water vapor was introduced with the olefin, to mimic the water concentration formed during the MTO reaction (i.e., the outlet partial pressure of water at 100% conversion of 10 kPa methanol). Identical to the experiments of toluene co-feeding, the total flow rate was unchanged, while the catalyst weight was systematically changed to reach different levels of conversions.

In the experiment addressing the impact of the carbon ratio of methanol to co-feed (butene or 0-pentene), experiments were performed in the 10-fold parallel reaction unit at 748 K with water dilution. 2-butanol or 2-pentanol were used as co-feed, as they were expected to be fully dehydrated on acidic zeolite to butenes and pentenes, respectively. Defining the carbon based concentration in a mixture of methanol and water (weight ratio 1:2) as 100%, different compositions of the same carbon based concentration were used: (a) 100 C% from methanol, methanol partial pressure 0.22 kPa, (b) 90 C% from methanol with 10 C% from co-feed (2-butanol or 2-pentanol), (c) 83 C% from methanol with 17 C% from co-feed (2-butanol or 2-pentanol), (d) 73 C% from methanol with 27 C% from co-feed (2-butanol or 2-pentanol), (e) 63 C% from methanol with 37 C% from co-feed (2-butanol or 2-pentanol), (f) 37 C% from methanol with 63 C% from co-feed 2-butanol. Thus, identical carbon concentrations were used in all experiments with alcohol co-feeds.

## 3. Results and discussions

### 3.1. Autocatalysis versus hydrocarbon pool proposal

Fig. 1 depicts the effect of repeated variations of the methanol contact time on the catalytic performance of a fixed catalyst loading. When a methanol conversion of 93% was reached at a contact time of 0.11 min kg<sub>cat</sub> mol<sub>MeOH</sub><sup>-1</sup>, the subsequent increase of flow rate led to a decrease of contact time to 0.03 min kg<sub>cat</sub> mol<sub>MeOH</sub><sup>-1</sup>,

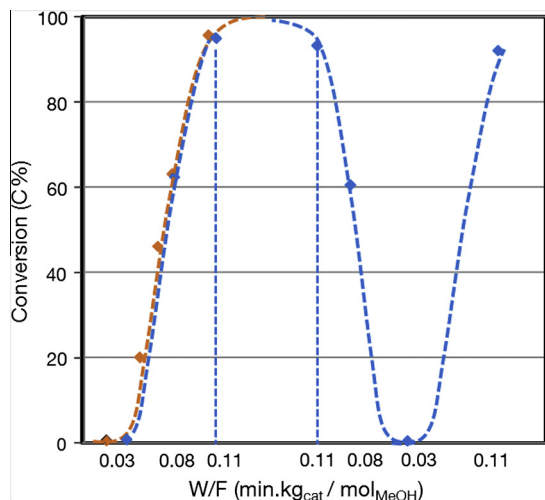


**Fig. 1.** Methanol conversion in repeated cycles by varying contact time at 723 K and methanol partial pressure of 10 kPa. Orange trace, data obtained varying the weight of fresh catalyst for a constant flow rate. Blue trace, data for a fixed catalyst charge at varying flow rates.

and the methanol conversion dropped to nearly zero. The following decrease of the flow rate brought the contact time back to  $0.11 \text{ min kg}_{\text{cat}} \text{ mol}_{\text{MeOH}}^{-1}$  and restored the methanol conversion to 93%. These repeated variations of flow rate led to fully reversible conversion cycles as shown in blue (Fig. 1) in accordance with the results of Olsbye et al. [5]. In addition, the results obtained with a fixed catalyst charge and varied flow rates overlapped with those obtained with a fixed flow rate and fresh catalyst of varied amounts.

This complete reversibility contradicts the strictest formulation of a hydrocarbon pool mechanism. According to this concept [17–19], it was believed that a surface carbon pool, which was supposed to be formed on the zeolite surface and to act as reservoir of centers when a high methanol conversion was reached, should have a longer residence time than the formed products [52]. If this were the case, the switch of contact time from 0.08 to  $0.03 \text{ min kg}_{\text{cat}} \text{ mol}_{\text{MeOH}}^{-1}$  should have generated an appreciable methanol conversion, one higher than the conversion obtained in the first experiment with a contact time of  $0.03 \text{ min kg}_{\text{cat}} \text{ mol}_{\text{MeOH}}^{-1}$ . This was clearly not observed. The conversion upon establishing a residence time of  $0.03 \text{ min kg}_{\text{cat}} \text{ mol}_{\text{MeOH}}^{-1}$  was nearly zero and the activity of a “pre-activated” catalyst was identical to that with a fresh catalyst (Fig. 1). The fully reversible conversion cycles indicate, therefore, that the carbon species are unstable, decomposing or desorbing rapidly as the flow rate is increased, and being formed rapidly after switching back to a higher residence time.

The indirect catalytic MTO cycle starts with the consecutive steps of methylation, the kinetics of which has been well described [44–50]. The widely accepted mechanism for methylation follows a mechanism, as depicted in Scheme 1, where a hydrocarbon molecule in the mobile phase (either olefin or aromatics) interacts with a chemisorbed methanol, i.e., methoxonium or methyl carbenium ion, and a methylated hydrocarbon is formed and desorbed [6]. The formed higher hydrocarbon molecules may undergo further reactions with other chemisorbed methanol molecules until the higher homologue has reached the size for which the rates of cracking on the acid site are higher than the rates of methylation. The reaction rate of methylation is reported to have a zero order and first order dependence on the partial pressures of methanol and hydrocarbons (olefin or aromatics), respectively [44–50]. This is in line with the general description for the rate of an autocatalytic reaction where the methanol conversion follows a characteristic S-shape as a function of contact time, as shown in

$$r = -k[M]^x[P]^y \quad (1)$$

where the  $[M]$  and  $[P]$  represent the concentrations of methanol and hydrocarbon products, respectively. Although the calculated reaction orders with respect to methanol deviate from zero and they are usually slightly below one at practical MTO reaction temperatures, it is well accepted that methanol adsorbs on the Brønsted acid sites of zeolite more strongly than light hydrocarbons. Therefore, the MTO mechanism can be seen as an analogue of the methylation mechanism depicted in Scheme 1. The zeolite surface is predominantly covered by methanol, and the hydrocarbon species has a significantly weaker interaction with zeolite than methanol. The Brønsted acid sites activate methanol molecules and are responsible for the final step of cracking of the highest hydrocarbon intermediates, acting as one type of catalytic center. On the other hand, the entrained lower hydrocarbons accommodate the “activated”  $\text{CH}_2$  entities, and the further cracking of the highest homologues produces the light olefins as products. The original lower hydrocarbon is regenerated in the meantime. In this way, the lower hydrocarbon, which is the starting point of a catalytic cycle, can be defined as another type of co-catalyst that offers a faster reaction route.

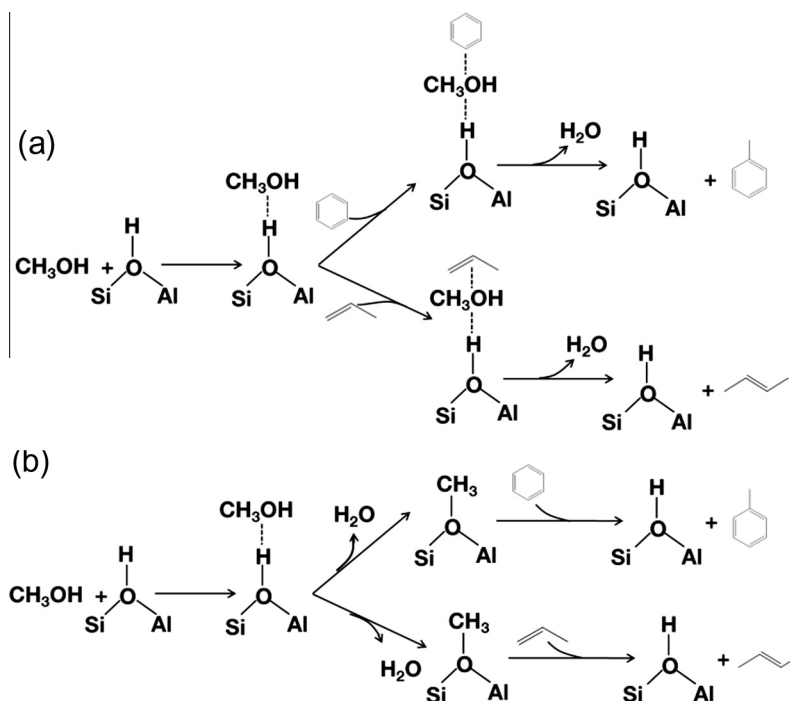
Therefore, the dynamic course of the interactions of zeolite (acid sites), hydrocarbon species, and methanol, demonstrated by the results obtained in the repeated cycles (Fig. 1), are better described by an autocatalysis mechanism, than by the original hydrocarbon pool proposal as shown in Scheme 2. Although both autocatalysis and hydrocarbon pool proposals rely on the critical roles of acid site and lower hydrocarbons (olefins or aromatics), the main distinction lies in the roles that the acid site and the hydrocarbons play. In the autocatalytic route, the acid site is covered predominantly by methanol and attacked by mobile-phase hydrocarbon; while in the strictest understanding of a hydrocarbon pool concept, the acid site adsorbs certain hydrocarbon species, constituting the reaction centers and then a surface pool of “ $-\text{CH}_2$ ” is formed via contributions by methanol, which split off gas phase light olefins as products.

Based on the above analysis of the description of the interactions between zeolite, hydrocarbons and methanol, we are now in a position to unify the autocatalysis and the hydrocarbon pool concepts. A generalized hydrocarbon pool mechanism should define the entrained hydrocarbons in the zeolite pores, other than the surface carbon species, as the working hydrocarbon pool species. Following this definition, hydrocarbon pool species, which are free of diffusional constraints, act also as entrained co-catalysts in the autocatalysis concept. Thus, a generalized hydrocarbon pool mechanism is at large in accordance with the autocatalysis concept, as long as one assumes a rapid exchange between the species adsorbed in the fluid phase of the zeolite.

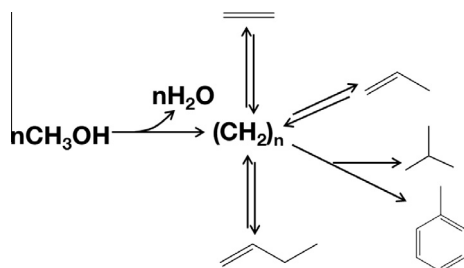
### 3.2. Insights from aromatics and olefin co-feeding

Based on the analysis in the previous discussion of the MTO mechanism on HZSM-5, methanol conversion proceeds via consecutive methylation reactions, in which the hydrocarbon species interact with the pre-adsorbed methanol. Therefore, competitive methylation of entrained aromatics and olefins in the zeolite pores will influence the locally prevalent hydrocarbons, which eventually propagate each specific cycle. Thus, the reacting molecules, except for methanol or dimethyl ether, need to remain, at large, in the mobile phase.

An increase in the abundance of aromatics in the feed leads to the selective propagation of the aromatics based cycle, especially at low methanol conversions. Therefore, compared to the conversion of the feed of pure methanol, propagation of the aromatics based cycle shifts the product distribution toward ethene and methylated aromatics. As *meta*-xylene has a larger kinetic



**Scheme 1.** Generally accepted mechanisms for methylation of aromatics or olefins, in which a gas-phase olefin or aromatic molecule reacts with a meth-oxonium ion (a) or methyl carbenium ion (b).



**Scheme 2.** Originally proposed hydrocarbon pool mechanism by Dahl and Kolboe [17–19].

diameter than the HZSM-5 zeolite pore, it cannot effectively diffuse into the channel to propagate the aromatics based cycle, which leads to a significantly smaller impact of such molecule in comparison with co-feeding *para*-xylene.

Further insight into the aromatics based cycle can be deduced from the experiments by co-feeding of toluene and benzene. As shown in Ref. [43], co-feeding toluene of the same molar concentration as *para*-xylene leads to an identical impact on the propagation of the aromatics based route. In other words, as shown in Fig. 2, toluene and *para*-xylene are both involved in one cycle as active intermediates and they play an identical role. This is due to the comparable diffusion coefficients and methylation rates for toluene and *para*-xylene. On the other hand, co-feeding benzene also leads to an identical degree of propagation of the aromatics based cycle, but it results in stoichiometrically more methylation of aromatics than that of toluene. As shown in Fig. 3, co-feeding 2 mol.% benzene led to 2% more ring methylation than the case of toluene co-feeding. This suggests that benzene itself is not an intermediate of the aromatics based cycle; however, the comparable rate coefficient for benzene methylation rapidly transformed benzene to toluene, which is actively involved in the cycle, as shown in Fig. 2.

Fig. 4(a) depicts the carbon-based product selectivities as a function of methanol/dimethylether conversion for a feed of

methanol and 4 mol.% *para*-xylene. At the lowest methanol conversion in this study, a carbon-based ethene selectivity of 39% and a propene selectivity of 36% were observed. Considering that ethene is very unreactive in further secondary reactions such as methylation or dimerization, and a small portion of propene is possibly methylated to higher olefins even at this low conversion, it is concluded that the aromatics based cycle, which has been found to be responsible for a dominant fraction of methanol conversion at low conversions, produces simultaneously ethene and propene with almost equal carbon-based selectivities.

This is further supported by the experiments adding aromatics at relatively low reaction temperatures. Fig. 5(a) and (b) depicts the aliphatic product distribution as a function of methanol conversion at 623 and 673 K, respectively, for a feed containing 4 mol.% *para*-xylene. It clearly shows that the extrapolated carbon based selectivities to ethene and propene are nearly equal at zero methanol conversion. This is in line with an observation by Bjørger et al. in which a HZSM-5 zeolite (Si/Al = 45) and a reaction temperature of 623 K were explored [51]. However, we note that the observation may be, in part, a result of transport effects. In an early report [52], Haag et al. stated that “With ZSM-5 catalyst of SiO<sub>2</sub>/Al<sub>2</sub>O<sub>3</sub> = 35–70, temperatures of 550–750 K and conversion as low as 0.05%, the molar ratio of propylene to ethylene was 1 or greater,” in agreement with our observation. However, in the same report using HZSM-5 with a SiO<sub>2</sub>/Al<sub>2</sub>O<sub>3</sub> = 1600 (which will have less transport effect on sequential reactions), the authors measured a propene to ethene ratio of <0.5 at a conversion <0.1 at 723 K and 1 bar. It is noted in the present study (Figs. 4a and 5) that the extrapolated selectivity to C<sub>4</sub><sup>+</sup> was less than 10% at zero methanol conversion. While reportedly it is feasible for C<sub>4</sub><sup>+</sup> to be formed by the aromatics based cycle as a minor product compared to ethene and propene, one cannot exclude the possibility that the olefin based cycle operates at extremely low conversion as a result of transport effects, contributing to the formation of a part of propene and C<sub>4</sub><sup>+</sup>. Considering the low carbon based amount of C<sub>4</sub><sup>+</sup> formed, we tentatively propose that the aromatics based cycle produces ethene and propene with equal carbon-based selectivities over HZSM-5 zeolites.

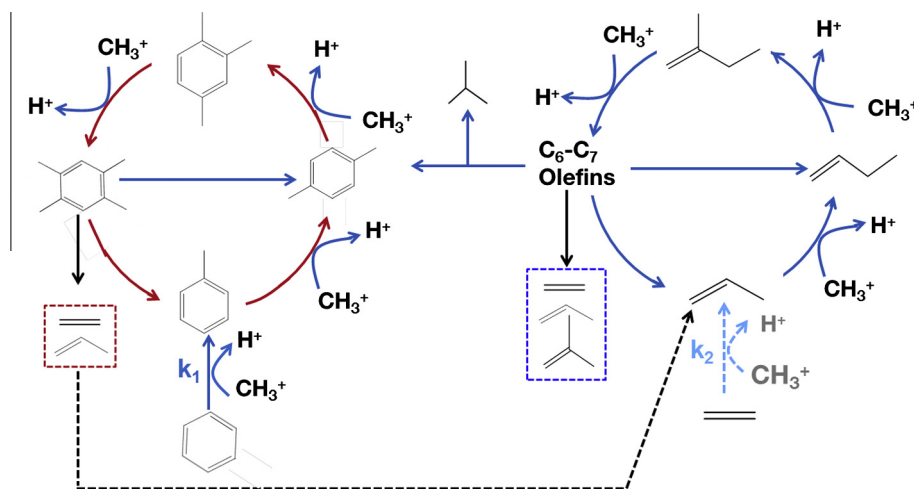


Fig. 2. A modified dual-cycle mechanism in operation during methanol-to-hydrocarbons catalysis over HZSM-5 under industrially relevant MTO conditions.

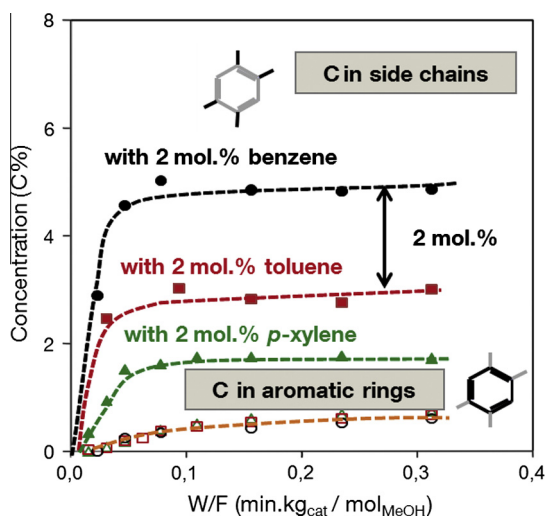


Fig. 3. Carbon distribution in the aromatic products by co-feeding methanol and benzene, toluene or para-xylene, in terms of carbon in the aromatic ring and carbon in the side chain. Methanol partial pressure was 10 kPa, aromatic co-feed partial pressure 0.2 kPa, reaction temperature 723 K. Durene, 1,2,4,5 tetramethylbenzene is illustrative of alkylated benzene products.

Although the olefin based cycle plays a minor role at low methanol conversions when aromatics are co-fed (as a result of the low concentration of olefins), the significance of the olefin based cycle increases with increasing methanol conversion. The explanation is that the aromatics based cycle produces ethene and propene in equal amounts. Propene is able to compete with aromatics and propagate the olefin based cycle at higher concentrations, resulting in the formation of most of the  $C_{3+}$  in the final product pool, as shown schematically in Fig. 2. For instance, in the experiment with a feed containing 4 mol.% *p*-xylene in which the aromatics based cycle is largely dominating, a maximum of 13 C% ethene is formed at nearly 100% methanol conversion ([43], Fig. 1(b)). If we make the extreme assumption that all ethene was formed by the aromatics-based cycle (note that the aromatics based cycle produces ethene and propene with equal carbon based rates), 13% methanol is then supposed to be converted concurrently to propene via the aromatics based route. Thus, less than 30% methanol is converted via the aromatics based cycle, and the remaining 70% methanol via the olefin methylation/cracking route. Therefore, although the aromatics based route dominates the initial conversions with a feed abundant in aromatics, the olefin based cycle is dominant during the overall conversion.

This is even more evident for the conversion of methanol in the absence of any co-feed. At very low conversion (below 0.1%), the

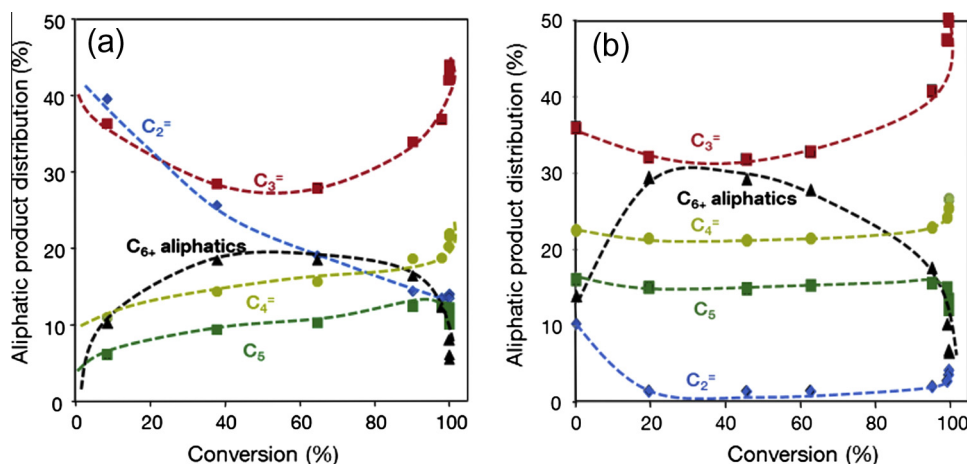


Fig. 4. Carbon-based  $C_{2+}$  aliphatic product distributions as a function of methanol/dimethylether conversion. Reaction temperature was 723 K, methanol partial pressure 10 kPa, para-xylene co-feed partial pressure (a) 0.4 or (b) 0 kPa.

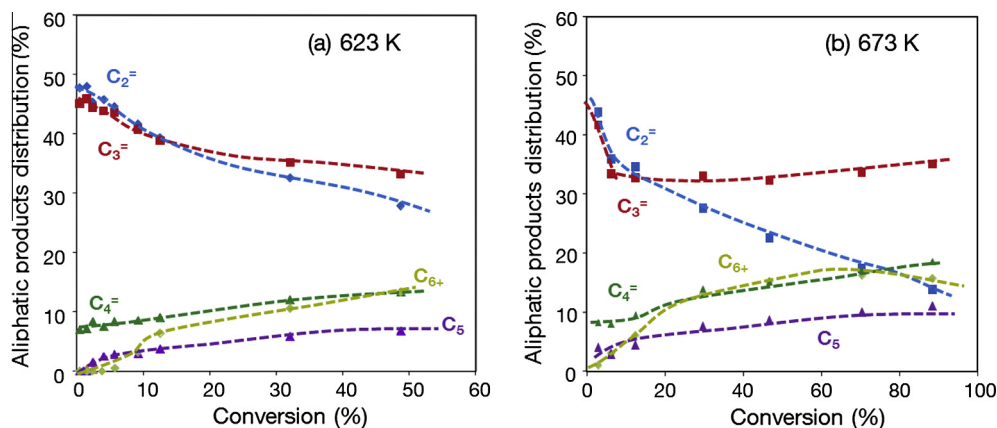


Fig. 5. Aliphatic product distributions versus methanol conversion with a feed of mixed methanol and toluene at reaction temperatures of 623 (a) and 673 K (b). Methanol partial pressure was 10 kPa, *p*-xylene co-feed partial pressure 0.4 kPa.

ratio of carbon selectivity of ethene to propene is close to one [51]. Therefore, the methanol conversion is proposed to be initiated by the aromatics based cycle. However, olefins formed will rapidly compete with the initial aromatic hydrocarbon species and the olefin based cycle will dominate the methanol conversion thereafter, as shown in Fig. 4(b).

Inspired by the finding that co-feeding identical concentrations of benzene, toluene or *para*-xylene led to the identical impact on the aliphatic product distribution, we designed similar experiments on the olefins based cycle by co-feeding various C<sub>2</sub>–C<sub>6</sub> olefins of the same carbon-based concentration. Indeed, very similar to the situation in the aromatics based cycle, it was demonstrated that co-feeding a lower concentration of olefins (up to 40 C% in this study) leads to product distributions independent of the identity of the co-fed C<sub>3+</sub> olefins at higher conversions [43]. As shown schematically in Fig. 2, similar to the roles that toluene and xylene play in the aromatics based cycle, C<sub>3</sub>–C<sub>6</sub> olefins take part in the olefin methylation/cracking cycle as active intermediates via rapid scrambling and incorporation of co-fed olefins by methylation and cracking with comparable rate constants. Adding ethene leads to the only exception. Contrary to benzene in the aromatics based cycle, ethene is not effectively involved in the olefin methylation/cracking and remains primarily unreacted, because it is at least one order of magnitude less active in methylation than C<sub>3+</sub> olefins (Fig. 2).

The observation that the final product distribution is independent of the nature of the co-fed olefins, strongly suggests that the olefin based cycle is the dominant reaction pathway on HZSM-5 under the studied reaction conditions (i.e., at higher conversions of methanol).

On the other hand, addition of olefins in the feed favors hydrogen transfer and aromatization. Even though the aromatics concentration is low compared to the olefins, aromatics have a relatively lower diffusion rate than the olefins. Therefore, these aromatics tend to stay in the pores and compete with olefins. In turn, the aromatics based hydrocarbon pool route remains active. The overall consequence is, therefore, that co-feeding olefins does not selectively propagate the olefin-based cycle. In other words, the ratio of activities of aromatics and olefins based cycles does not significantly change compared to that in the case of a pure methanol feed.

### 3.3. Comparison with olefin cracking

At this point we have shown that two distinct catalytic cycles operate over HZSM-5, with the olefin methylation/cracking route being the dominant reaction pathway in the overall methanol conversion range, and that the final product distribution under typical

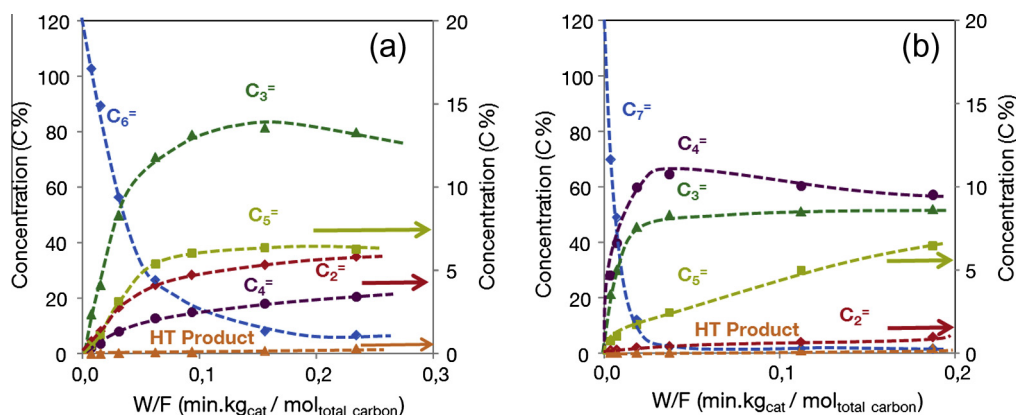
MTO reaction conditions is dictated to a large extent by C<sub>6</sub>–C<sub>7</sub> olefin cracking. Therefore, to gain mechanistic insight into olefin transformations within the complex chemistry involved, the conversion of pure olefins, i.e., 1-hexene and 1-heptene, was studied at reaction conditions as close as possible to those industrially practiced in the MTO reaction. As water is formed during the MTO reaction, 10 kPa water vapor (i.e., the outlet partial pressure of water at 100% conversion of 10 kPa methanol) was introduced with the olefin.

Fig. 6 illustrates the conversion of 1-hexene and 1-heptene of the same concentration of 120 C% (equivalent to the 120% carbon form a feed containing 100 C% of methanol and 20 C% from olefin co-feed, but no actual methanol in the feed), respectively, as a function of contact time. Different from the previous sections, the contact time in this section is defined as the ratio of carbon molar flow rate to catalyst weight, with units of  $\text{min kg}_{\text{cat}} \text{mol}_{\text{total carbon}}^{-1}$ .

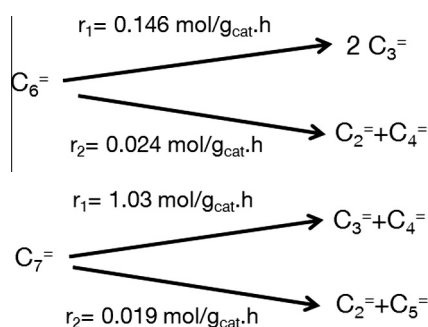
The primary reactions of 1-hexene cracking proceed via two pathways, forming ethene and butene (1:1) as well as two molecules of propene, respectively (Scheme 3). As shown in Fig. 6, the former primary reaction is much slower than the latter. The ratio of the reaction rates for these two primary reactions was estimated to be 6, based on the selectivities to propene and ethene at the lowest contact time studied (Table 1). Fast secondary reactions of propene, which was the main product, with 1-hexene, which was abundant at low conversions, led to butenes and pentenes, resulting in the deviation of butenes and ethene from unity, even at the lowest contact time studied. In the case of 1-heptene, the predominant cracking route leads to propene and butenes, essentially in accord with the stoichiometry (Fig. 6 and Table 1). Other products were formed with very low selectivities even at 1-heptene conversion of 42%. The much faster primary cracking of 1-heptene than that of 1-hexene might be the reason as to why propene and butenes were observed in parity at 1-heptene conversion of 42%, while the ethene/butenes ratio deviated from unity when 1-hexene conversion was still 10–20%.

At longer contact times, the primary olefin products undergo reactions with the reactant and among themselves, resulting in an increased formation of olefins, which would not be expected from monomolecular pathways mediated by carbenium ions, e.g., pentenes from cracking of 1-hexene. Hydrogen transfer reactions between olefins become detectable with increasing conversion, but the extent remains very low.

Three groups of products, i.e., propene, ethene and hydrogen transfer products (C<sub>2</sub>–C<sub>4</sub> light alkanes plus aromatics), deserve special attention in the context of comparing the catalytic performance of HZSM-5 in olefin cracking (pure olefin feeds) and the



**Fig. 6.** Reaction pathway for 1-hexene (a) and 1-heptene (b) cracking at 723 K. Water partial pressure 10 kPa, partial pressures for 1-hexene and 1-heptene were 2 and 1.7 kPa, respectively. For the sake of comparison, 1-hexene and 1-heptene were expressed as 120% C. Hydrogen transfer (HT) products include aromatics and C<sub>2–4</sub> paraffins.



**Scheme 3.** Primary reaction routes for 1-hexene and 1-heptene cracking. Reaction rates based on the product distribution at the lowest conversion measured.

MTO reaction (methanol-olefin mixtures). Analysis of these products can also provide valuable information about the olefin methylation/cracking route. At full reactant conversion, 1-hexene cracking led to a higher concentration of propene, while 1-heptene cracking led to a lower propene yield compared to the propene produced from the methanol and C<sub>3–6</sub> olefin reaction mixture (Fig. 7).

This agrees well with the olefin methylation/cracking mechanism for mixed methanol-olefin feeds, in which olefin methylation either terminates at hexenes that are cracked to propene or terminates at heptenes that are cracked to propene and butenes (one heptene molecule produces one propene molecule). The fact that the propene yield from mixed methanol-olefin feeds was closer to that from 1-heptene cracking suggests a higher termination probability at heptenes for the conversion of methanol in the presence of co-fed C<sub>3–6</sub> olefins. Note that 100% conversion of methanol occurs at a specific residence time of about 0.12 min kg<sub>cat</sub>/mol<sub>total carbon</sub>, see Fig. 8, so the comparison is appropriate at or beyond this point.

C<sub>1–4</sub> alkanes and aromatics that are referred to as hydrogen transfer (HT) products in this work are undesirable in the MTO

process. Fig. 8 depicts the yield of these HT products, as a function of contact time, for the methanol-olefin feed (molar ratio = 100:20) and various pure C<sub>5–7</sub> olefin feeds with the same total carbon concentration. Over the whole range of contact time, hydrogen transfer was significantly higher for the methanol-containing feed compared to pure olefin feeds. Upon reaching full conversion of methanol, the formation rates of the HT products from the methanol-containing feed and pure olefin feeds became comparable, as indicated by the similar slopes at higher contact times. These HT products were possibly formed via reactions between two olefin species, which should be similar for both cases, as both methanol and higher olefins were converted predominantly to C<sub>3–5</sub> olefins at full reactant conversions.

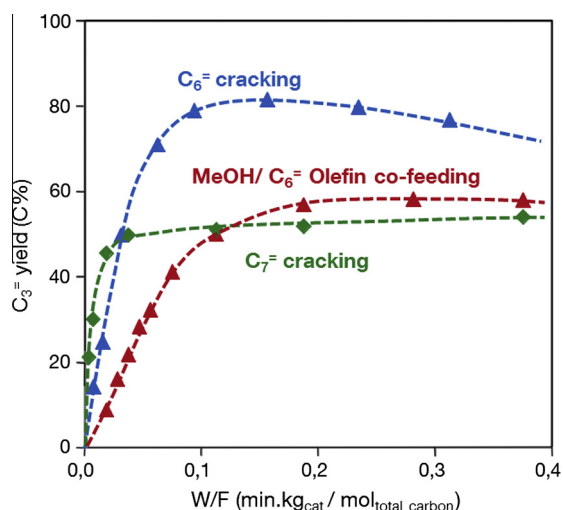
Before full conversion of methanol, hydrogen transfer proceeded much faster in the methanol-olefin mixed feed than in pure olefin feeds. Although a molecular-level understanding of the hydride transfer routes is only beginning to emerge, the results demonstrate clearly that a hydrogen transfer pathway exists, which involves methanol or intermediates derived from it and which has a higher rate than the one along the classical route between two olefinic species.

Fig. 9 depicts the yield of ethene as a function of contact time from four different feeds, including a methanol-olefin mixed feed (the choice of C<sub>3–6</sub> olefin does not impact the product distribution), 1-pentene, 1-hexene and 1-heptene. Before reaching >90% conversion, 1-hexene cracking gave rise to the highest formation rate of ethene among all four feeds, indicating that the kinetically primary cracking of 1-hexene to ethene and butenes dominates under realistic MTP reaction conditions. Ethene formation from 1-pentene cracking was the second highest, while 1-heptene cracking produced ethene in a much lower rate and yield over the studied range of contact times. From the yield ratio of formed ethene, propene and butenes, it is concluded that the bimolecular reaction pathway (that is, methylation/cracking of CH<sub>3</sub>OH + C<sub>n+1</sub> to produce C<sub>n</sub> + ethene) plays a predominant role in the formation of ethene, which is essentially formed by cracking of secondary products such as

**Table 1**

Conversions and product distributions at low contact times for cracking of 1-pentene or 1-hexene or 1-heptene. Reaction temperature was 723 K. Partial pressure of water vapor was 10 kPa, and partial pressures for 1-pentene, 1-hexene or 1-heptene were 2.4, 2 and 1.7 kPa, respectively, leading to an equivalent 120 C% in each feed mixture (referred to as the 120 C% from a feed containing 100 C% of methanol and 20 C% from the co-fed olefin). The conversion rates were given on a molecular basis.

Feed	Conversion rate (mol g <sub>cat</sub> <sup>-1</sup> h <sup>-1</sup> )	Conversion (%)	Hydrocarbons (C%, in total 120 C%)					
			C <sub>2</sub>	C <sub>3</sub>	C <sub>4</sub>	C <sub>5</sub>	C <sub>6</sub>	C <sub>7+</sub>
1-C <sub>7</sub>	1.05	41.9	0.15	21.15	28.0	0.71	0.25	69.74
1-C <sub>6</sub>	0.17	14.5	0.76	14.20	1.93	0.51	102.59	
1-C <sub>5</sub>	0.02	1.6	0.22	0.55	0.43	118.15	0.65	



**Fig. 7.** Propene yield as a function of contact time for the feeds of 1-hexene, 1-heptene, and methanol co-fed with 20%  $C_{3-6}$  olefins. Total concentration of carbon was 120% for all feeds. Reaction temperature 723 K. For cracking of 1-hexene and 1-heptene, water partial pressure was 10 kPa, and partial pressures for 1-hexene, and 1-heptene were 2 and 1.7 kPa, respectively.

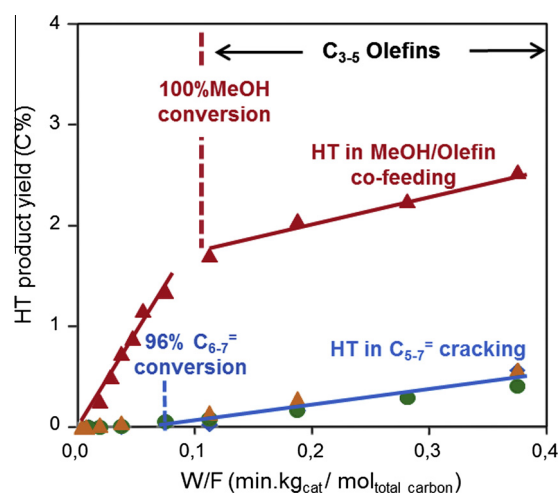


**Fig. 8.** Yield of hydrogen transfer products as a function of contact time for the mixed feeds containing methanol (100%) and 1-pentene, 1-hexene and 1-heptene (20%). Reaction temperature 723 K.

hexene cracking [53] (Scheme 3). Compared to hexene cracking, the ethene formation rate from the methanol-olefin feed was lower. This implies that under realistic reaction conditions (methanol total conversion), hexene cracking acts as an important route for ethene formation. Analogous to the situation for the hydrogen transfer rates, with contact times longer than 0.1 min  $\text{kg}_{\text{cat}} \text{mol}_{\text{MeOH}}^{-1}$  the ethene formation showed an identical rate independently whether the feed was methanol,  $C_6$ , or  $C_7$ . This again was attributed to the similar actual feed composition after cracking, predominantly  $C_{3-4}$  olefins ( $\geq 85\%$ ). Therefore, ethene is concluded to be formed from the oligomerization of lower olefin and the subsequent cracking of  $C_6$  intermediates. The only exception is ethene formation from  $C_5$ . At a contact time of 0.11 min  $\text{kg}_{\text{cat}} \text{mol}_{\text{MeOH}}^{-1}$ , which has been sufficient to almost fully convert the other feeds (conversion  $\geq 96\%$  for  $C_{6-7}$  and 100% for methanol), the overall pentene conversion was only 32%. Therefore, the actual feed composition from 1-pentene behaves very differently from the others and it forms increasing amounts of ethene as the contact time is extended and further pentene conversion is achieved.

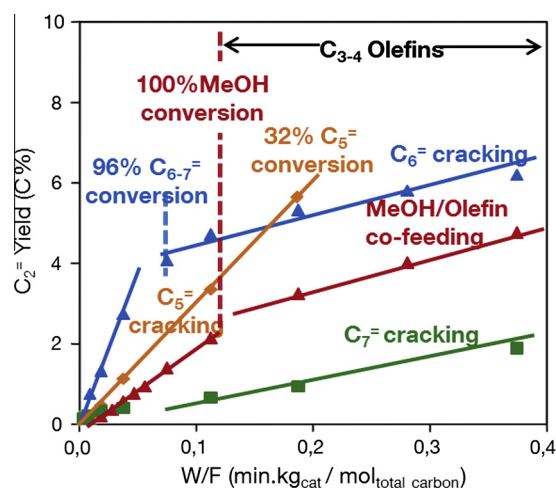


**Fig. 9.** Yield of ethene as a function of contact time for the feeds containing methanol (100%) and 1-pentene, 1-hexene, and 1-heptene (20%). Reaction temperature 723 K, water partial pressure 10 kPa; partial pressures for 1-pentene 1-hexene and 1-heptene: 2.4, 2.0 and 1.7 kPa, respectively.

It should be emphasized that the main conclusion drawn from Fig. 9, i.e., that hexene cracking is an important route for ethene, is apparently against the proposal widely accepted in literature that ethene does not form via the olefin methylation and cracking cycle, but via the aromatics based cycle, as demonstrated by the isotope experiments by Bjørger et al. [37,38]. However, a detailed comparison of the reaction conditions shows that the reaction temperature (623 K) for most mechanistic studies [37,38] is much lower than the typical temperature range (723–773 K) for MTO and MTP processes, which leads to the different product dependencies. It is, thus, concluded that the reaction temperature is the key factor affecting the dominant formation pathway for ethene. The olefin based route,  $C_6$  cracking as the key step, has a significantly higher activation energy than the aromatics based cycle. Therefore, although ethene predominantly forms via the aromatics based cycle at lower reaction temperatures such as 623 K, the olefin based cycle is the most significant pathway at 723 K and above.

This conclusion about the formation route of ethene via  $C_6$  olefin cracking is supported by the impact of reaction temperature on the MTO product distributions, as shown in Fig. 10. With the increase of reaction temperature, both yields of ethene and propene increased. Correspondingly the yield of  $C_{4+}$  aliphatics decreased with temperature. This indicates that the higher olefin cracking at higher reaction temperatures is the main reaction route that leads to the favored formation of light olefins. Most importantly, the yield of hydrogen transfer products decreased with reaction temperature, most probably due to a lower coverage of olefinic species at higher temperature. The opposite trends of ethene and aromatics demonstrated that much of ethene is mechanistically not linked with aromatics, but comes from the other pathways, i.e.,  $C_6$  olefin cracking.

#### 3.4. Impact of methanol to olefin co-feed ratio on product distribution

The finding that the product distribution is independent of the nature of the co-fed  $C_{3-6}$  olefin contradicts the observation of a remarkable impact of the identity of co-fed olefins by Xiao et al. [53]. The authors applied identical partial pressures of methanol and co-fed  $C_{2-6}$  olefin, corresponding to C-based olefin-to-methanol ratios of (2–7):1, which is significantly higher than those applied in this work (at most 4:10) [53]. Similarly, it was observed that 1-butene and 1-pentene, when co-fed with methanol in a C-based ratio of 1:1, influenced the product distribution (Fig. 11). A

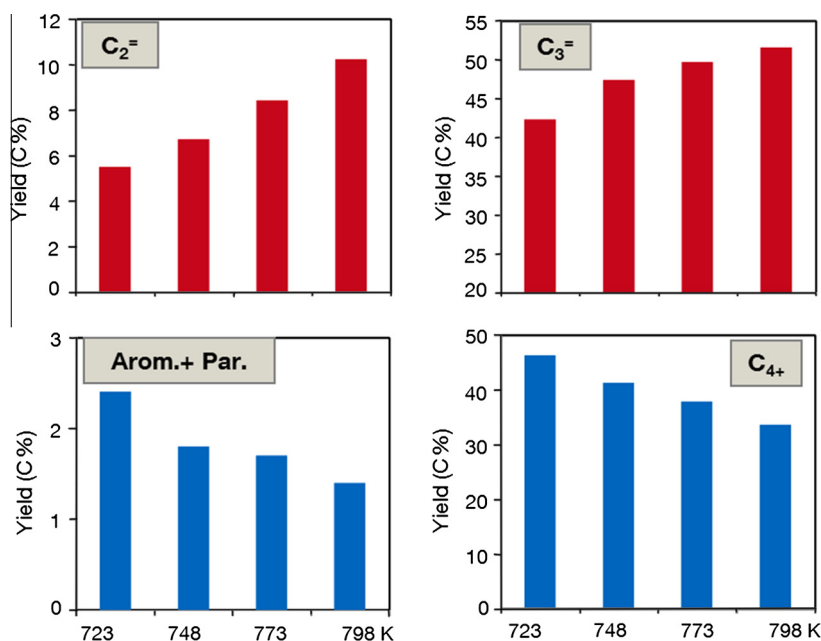


Fig. 10. Impact of reaction temperature on the MTO product distribution over HZSM-5. Methanol partial pressure was 22 kPa, diluted by water.

similar or even higher concentration of olefin co-feed relative to methanol is inferred to lead to a more effective competitive adsorption by the olefin-derived species and a greater fraction of methanol being consumed by methylation of such olefin-derived species. In this case, the product distribution at complete methanol conversion is dominated by the subsequent inter-conversion of the formed higher olefins, which reflects the impact of the nature of co-fed olefin. In contrast, when only a small fraction of olefin is co-fed with methanol, the catalyst surface is dominated by methanol-derived species, which are, in turn, responsible for the major part of methanol consumption. Fast olefin methylation/cracking leads to scrambling of co-fed carbon in the products, and, thus, the product distribution becomes independent of the co-feed identity.

To investigate the effect of the feed composition on the product distribution, different feeds of an identical total carbon concentration were studied. Defining the carbon based concentration as 100% in the mixture of methanol and water with a weight ratio 1–2, they were (a) 100 C% from methanol, methanol partial pressure 0.22 kPa, (b) 90 C% from methanol with 10 C% from co-feed (2-butanol or 2-pentanol), (c) 83 C% from methanol with 17 C% from co-feed (2-butanol or 2-pentanol), (d) 73 C% from methanol with 27 C% from co-feed (2-butanol or 2-pentanol), (e) 63 C% from methanol with 37 C% from co-feed (2-butanol or 2-pentanol), (f) 37 C% from methanol with 63 C% from 2-butanol, respectively, and the product distributions at 100% methanol conversion are depicted in Table 2. Less methanol in the feed led to a lower concentration of methane, while identical yields of ethene were observed, irrespective of the feed composition. A decrease of the methanol concentration in the feed from 100 C% to 63 C% led to little change in  $C_{2+}$  production distribution, and at a fixed methanol concentration, the product distribution was independent of the nature of the co-feed. The yield of  $C_{2-4}$  paraffins and aromatics decreased with decreasing concentration of methanol. While the amount of methane was about an order of magnitude lower, its correlation with  $C_{2-4}$  paraffins and aromatics suggests that it can be viewed as a less probable hydride transfer product. Further decrease in the methanol concentration to 37% significantly shifted the product spectrum from propene to butenes and  $C_{5+}$  aliphatics.

These results are consistent with the other findings in this work. A decrease of the methanol concentration from 100% to 63% did not essentially alter the surface chemistry, which was still dominated by the presence of methanol/dimethyl ether and its derived  $C_1$  entities, and the olefin methylation/cracking route resulted in a similar product distribution for the nine feeds (100 C% methanol, 90 C% methanol + 10 C%  $C_4$  or  $C_5$ , 83 C% methanol + 17 C%  $C_4$  or  $C_5$ , 73 C% methanol + 27 C%  $C_4$  or  $C_5$ , 63 C% methanol + 37 C%  $C_4$  or  $C_4$  and  $C_5$ ). However, a further decrease of methanol concentration in the feed to 37% results in competitive adsorption of the methanol and 1-butene species. Therefore, analogous to the case shown in Fig. 11, a separate methylation and olefin cracking reaction path will lead to a product distribution different from that resulting from a methanol dominated hydrocarbon pool route. With an identical carbon concentration in the feed, the feed containing 100 C% methanol showed the highest yield of hydrogen transfer products (including methane), as the methanol-involving hydrogen transfer pathway has a higher rate than the classical route, which solely involves olefins (Fig. 8). Although the yield of aromatic products decreased from 1.5% to 1.0% when the concentration of methanol in the feed decreased from 100% to 63%, the yield of ethene remained very similar (6.9% compared to 7.0%). This indicates again that at an elevated reaction temperature of 748 K, ethene is hardly mechanistically linked with the presence of aromatic molecules, and the olefin cracking route becomes an important pathway for ethene formation.

### 3.5. Toward elucidating the working mechanism in MTO over HZSM-5

As outlined before, the dual cycle concept [38] depicts the key reaction steps including olefin methylation and cracking, aromatics methylation and dealkylation, and hydrogen transfer as a bridging step [6]. In the context of elucidating the effect of the zeolite topology, reaction conditions and practical operations on the final product selectivity, more quantitative descriptions of the individual reaction steps of the dual cycle mechanism are, while crucial, yet to be fully developed.

Two key persistent questions are for a specific cycle, (1) what influences the intrinsic selectivities to the desired products and (2) what accounts for the formation of and what is the nature of

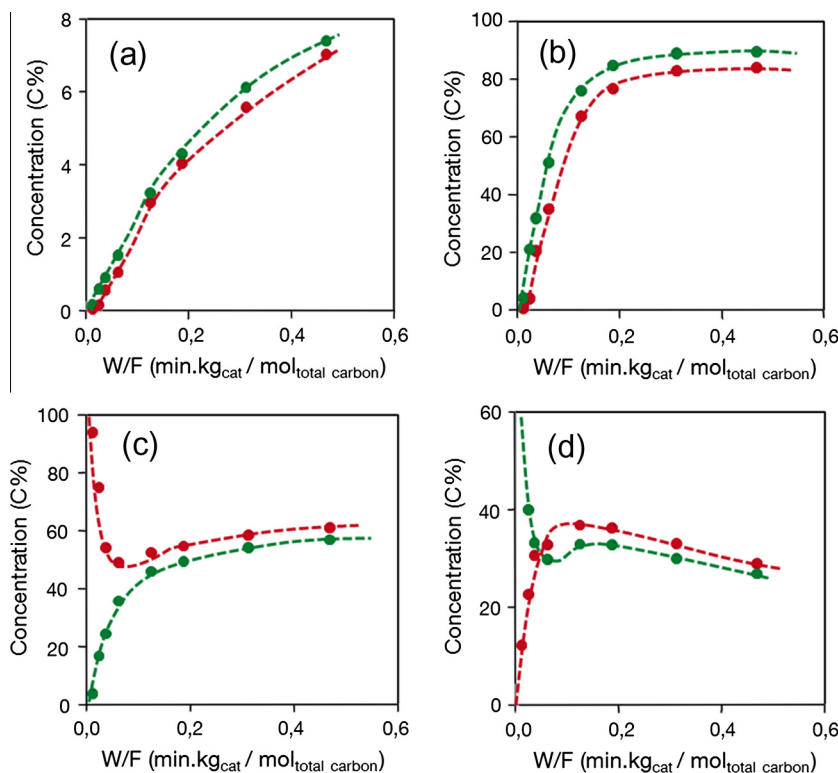


**Fig. 11.** Concentrations of products ethene (a), propene (b), butenes (c) and C5 hydrocarbons (d), as a function of contact time for feed mixtures containing 100 C% methanol and 100 C% from 1-butene (in red) or 1-pentene (in green). Reaction temperature 723 K, methanol partial pressure 10 kPa, and partial pressures for 1-butene and 1-pentene 2.5 and 2 kPa, respectively (equivalent to 200 C% in each feed mixture).

**Table 2**  
Detailed product distributions as a function of feed composition. Carbon based concentration was defined as 100% in the mixture of methanol and water with a methanol partial pressure of 22 kPa. Reaction temperature 748 K, weight hourly space velocity with respect to carbon was  $0.56 \text{ g}_{\text{carbon}} \text{ g}_{\text{cat}}^{-1} \text{ h}^{-1}$ .

Feed composition (%C)			Product distribution (%C)						
Methanol	2-Butanol	2-Pentanol	C <sub>1</sub>	C <sub>2</sub>	C <sub>3</sub>	C <sub>4</sub>	C <sub>5+</sub>	C <sub>2</sub> –C <sub>4</sub> paraffins	Aromatics
100	0	0	0.35	6.9	46.9	26.7	14.5	2.8	1.5
90	10	0	0.27	6.9	46.9	26.7	14.6	2.7	1.4
90	0	10	0.27	6.9	46.9	26.7	14.6	2.7	1.4
83	17	0	0.23	6.9	47.0	27.0	14.6	2.6	1.3
83	0	17	0.23	7.0	47.0	27.0	14.6	2.6	1.3
73	27	0	0.17	6.9	47.0	27.0	14.6	2.5	1.2
73	0	27	0.18	6.9	47.0	27.0	14.6	2.5	1.2
63	37	0	0.14	7.0	47.1	27.2	14.7	2.5	1.0
63	20	17	0.15	7.1	47.0	27.1	14.9	2.4	1.0
37	63	0	0.08	7.0	44.1	30.2	15.3	2.3	0.6

the prevalent active hydrocarbon species? The complex chemistry of methanol conversion makes it challenging to answer these questions unequivocally. The key information, which has been derived from the present study over HZSM-5 includes, however, several points. The aromatics based cycle operates over HZSM-5 and produces ethene and propene with carbon-based intrinsic selectivities of 1 to 1 at realistic reaction temperatures for the MTO process. The olefin based methylation/cracking route dominates. Growth of the carbon chain terminates predominantly at C<sub>6</sub> or C<sub>7</sub>. The subsequent cracking of these higher olefins via carbenium ions and β-scission leads to a product spectrum significantly more selective to propene and C<sub>4+</sub> than to ethene. An estimate from C<sub>6–7</sub> olefin cracking demonstrated that the relative ratio of carbon based selectivities for ethene to propene is 5–100.

The final product distribution, however, depends not only on the intrinsic selectivities for a specific cycle, but also relies to a large extent on the methanol conversion to which each of the

catalytic cycles contributes. The turnover rate for an aromatics- or olefin-populated site has still not been assessed. It should be noted, however, that the olefin based route is by far the dominant reaction pathway at high methanol conversion, and its significance increases with methanol conversion to olefins.

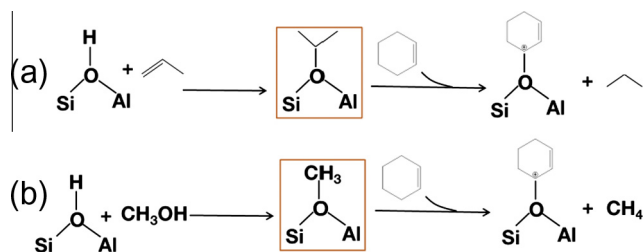
Let us turn at this point to the dominant pathway of ethene and propene formation on HZSM-5. It has been shown that the olefin based cycle dominates in methanol conversion over HZSM-5 irrespective of the co-feed. Combined with the fact that this cycle is highly selective toward C<sub>3+</sub>, it allows us to conclude that C<sub>3+</sub> olefins are predominantly formed from the olefin based cycle. The formation route of ethene, on the other hand, is more complex, and depends on multiple parameters. For a feed rich in aromatics, the aromatics based cycle is selectively promoted, and correspondingly it acts as the dominant pathway for ethene formation. However, for the conversion of feeds of methanol with or without olefin co-feeds, ethene is formed via aromatics and olefin based catalytic

cycles. In this case, the reaction conditions critically influence the relative contributions of the two pathways. This is related to the fact that the aromatics based cycle is comparatively more selective in ethene formation, but it contributes significantly less to methanol conversion, especially at high conversions. On the other hand, the olefin based route is significantly less selective to ethene formation, but the olefin driven autocatalysis makes it overwhelmingly active in converting methanol, the selectivity to ethene increasing with increasing reaction temperature. Therefore, the contribution for each cycle depends on the methanol conversion and reaction conditions. At low methanol conversions and relatively low reaction temperatures, a large fraction of ethene is formed via the aromatics based cycle. However, the olefin based cycle contributes more significantly to the ethene formation as the methanol conversion and reaction temperature increase.

The present results clearly identify the cracking of olefinic intermediates as the dominant reaction pathway in the MTO conversion over HZSM-5 catalysts. However, particular attention was paid to the critical role that methanol and methanol/olefin ratio feeds play in the reactions.

As shown in the Section 3.3, a hydrogen transfer pathway involving methanol or surface reaction intermediates directly derived from methanol have a much higher rate than the classical route between two olefinic species. We tentatively propose that this pathway is linked with intermediates of the chemisorbed methanol (Scheme 4(b)), which can undergo a reaction analogous to the reaction proposed for surface species derived directly from an acid site adsorbed olefin (Scheme 4a). As methanol derived species is believed to have a significantly higher coverage than the olefin products due to a high adsorption ability, the methanol-involved hydrogen transfer pathway would be very important at partial methanol conversions. It is proposed that the reaction would lead to the formation of methane and a more unsaturated cyclic species (cyclohexadiene-like) which is in turn more active than cyclohexene in participating in other hydrogen transfer reactions. This is supported by the fact that less methanol in the feed led to less hydrogen transfer products including methane, C<sub>2–4</sub> paraffins, and aromatics, as shown in Table 2.

Along with this proposal, it is indicated that the conversion of methanol produces light olefins and hydrogen transfer products in parallel reactions pathways. This is in line with a long-standing observation in the MTH conversion [54]. The C<sub>4</sub> Hydrogen Transfer Index (C<sub>4</sub> HTI) is often used in methanol chemistry to describe the hydrogen transfer activity. The C<sub>4</sub> HTI is defined as the ratio of C<sub>4</sub> paraffin (*n*-butane and iso-butane) concentration to the total C<sub>4</sub> concentration. A high C<sub>4</sub> HTI indicates a high activity in converting olefins to aromatics and alkanes. Fig. 12 depicts the plot of C<sub>4</sub> HTI as a function of methanol conversion. The C<sub>4</sub> HTI remains almost unchanged over a wide range of methanol conversion, indicating a constant hydrogen transfer activity. This implies that olefin formation and hydrogen transfers proceed in parallel rather than in sequential reactions. This would not have been the case, if



**Scheme 4.** Proposed mechanistic pathway for the methanol enhanced hydrogen transfer via the same intermediate as olefin formation via methylation.

hydrogen transfer solely occurred between olefins (see the envisioned curve in Fig. 12 to guide the eyes). The reason is that the concentration of olefins increases with increasing methanol conversion, and, thus, hydrogen transfer between secondary products would necessarily lead to a significant increase of C<sub>4</sub> HTI with increased methanol conversion.

Inspired by the unique role that methanol plays in the hydrogen transfer reactions, which are responsible for the formation of coke precursors, we turn at this point to the impact of methanol on the catalyst deactivation. Fig. 13 depicts the evolution of concentrations of methanol and C<sub>2–4</sub> olefins as a function of time on stream for the various methanol containing feeds (100%, 90%, 83%, 73%, 63% methanol, respectively). The identical total carbon concentrations (100 C%) were ensured by adding required concentrations of *n*-butanol correspondingly. Independent experiments showed that the co-fed *n*-butanol had an extremely high dehydration activity under the employed test conditions; therefore *n*-butanol was expected to be fully dehydrated on acidic zeolite to butenes over the very top layer of the catalyst bed (less than 2 mg of the total 300 mg catalyst bed loading). As shown in the Section 3.4 and Table 2, conversion of the five feeds produces identical olefin distributions at the initial time on stream. However, as shown in Fig. 13, a substitution of 10% methanol by higher alcohol (butanol) resulted in a doubled catalyst lifetime (lifetime was defined as the time on stream when the methanol concentration in the reactor effluent reached 10%). A further increase of the butanol concentration to 17 C% or even higher concentrations in the feed led to a substantially longer catalyst lifetimes. This is generally in line with the observations that less methanol in the feed resulted in less aromatic products. However, the slight decrease of the yield of aromatic products (1.5% compared to 1.4%) can hardly be associated with the doubled lifetime when 10 C% butanol was co-fed, clearly indicating the existence of another deactivation pathway involving methanol.

As shown in Table 2, the main distinction in the product distributions is the yield of methane. 10 C% butanol in the feed led to an appreciably lower methane formation. As illustrated in Scheme 4, methane is proposed to form via reduction of a methyl group by hydride transfer. Generally in line with an early proposal [55], we propose that methanol itself acts as the hydride donor during the initial phase when no or little olefin species exist, leading to the formation of methane and formaldehyde, as shown in Scheme 5a. The reactive formaldehyde molecules may undergo

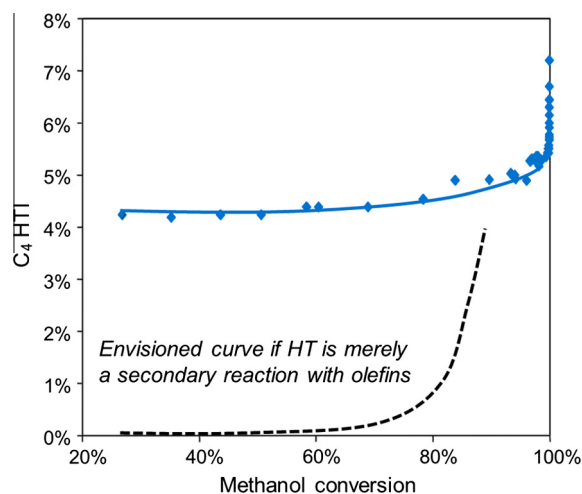


**Fig. 12.** C<sub>4</sub> Hydrogen Transfer Index (C<sub>4</sub> HTI) as a function of methanol conversion. Methanol partial pressure was 22 kPa, diluted in water. Reaction temperature 748 K.

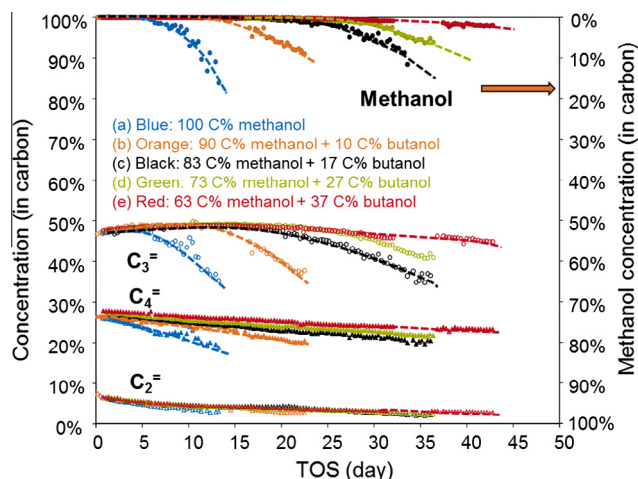


**Fig. 13.** Concentrations of methanol and  $C_{2-4}$  olefins as a function of time on stream for feeds (all diluted in water) of (a) 22 kPa methanol, (b) 19.8 kPa methanol and 0.55 kPa 2-butanol, (c) 18.2 kPa methanol and 0.94 kPa 2-butanol, (d) 16 kPa methanol and 1.48 kPa 2-butanol, (e) 13.8 kPa methanol and 2.1 kPa 2-butanol, respectively. All feeds contained the identical carbon based concentration. Reaction temperature 748 K, weight hourly space velocity  $0.56 \text{ g}_{\text{carbon}}^{-1} \text{ h}^{-1}$ .

Formose-type reactions leading to carbon–carbon formation and chain growth and further dehydrations (Scheme 5b). This results in the formation of the first cyclic species, as depicted in Scheme 5b. This hetero-atom unsaturated cyclic species aggregate further, forming the coke (Type-1 deactivation species) which can rapidly deactivate the acid site due to its high sticking affinity [55]. Further work is currently on-going for a detailed kinetic and physiochemical analysis of the formation of coke. Such reaction pathway might in fact be able to initiate and/or enhance the aromatics based cycle, which in turn forms the first olefin products. The formed olefins then compete with the hydride transfer pathway depicted in Scheme 5a in reacting with methanol via the rapid, “autocatalytic” olefin based cycle at an overwhelmingly higher rate. On the other hand, aromatic molecules are subsequently formed via hydrogen transfer. The adsorption of these aromatic coke precursors and further transformation leads to the formation of the classic “graphitic” coke (Type-2 deactivation species), typically observed on deactivated MTO catalysts.

Along with this proposal, it is speculated that when a 100% methanol feed was used in the plug-flow reactor, the active catalyst layer on the very top is in contact with only methanol, which leads to the formation of coke (Type 1 deactivation species) and subsequently a fast deactivation of this catalyst layer. With time on stream, the whole catalyst bed deactivates and layer by layer

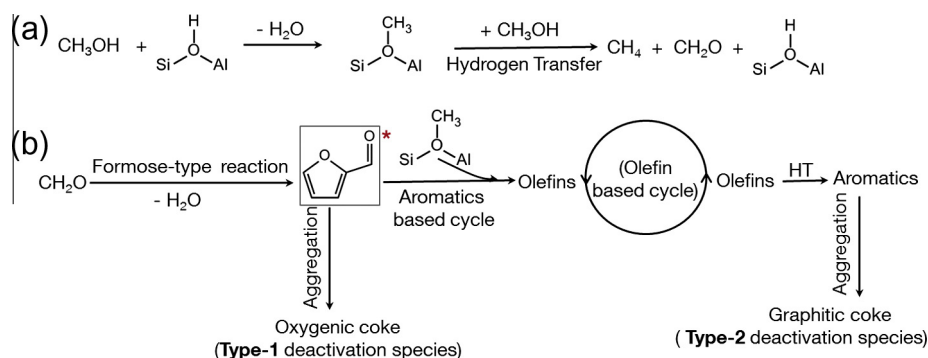
from top down mainly via this type of mechanism. However, when small concentrations of higher olefin (or alcohol) were co-fed, the deactivation pathway described above is largely bypassed, because the olefin based cycle would compete with a rate overwhelmingly faster than the rate of the pathway depicted in Scheme 5a, leading to little formation of the oxygenic coke. In the case of feed with high content in olefins or alcohols, the main coking species is expected to be the graphitic type (Type-2 deactivation species). This graphitic coke is formed and deactivates the catalyst in a relatively much lower rate compared to the oxygenic coke. This accounts for the significantly longer catalyst lifetime achieved when small amounts of a higher alcohol (olefin) are co-fed (Fig. 13).

To summarize, we conclude that when a pure methanol feed is used, the aromatic based cycle starts. The first aromatic species is proposed to be formed via oxygenic  $C_1$  species. This proposal allows the interpretation of the observation that at extremely low conversion, methane is the major hydrocarbon formed in line with earlier observations of Haag et al. [52]. At still lower conversion (0.05%) of a pure methanol feed, the main products were methane (85%), and ethane and propene selectivity was close to 1.

#### 4. Conclusions

The MTO reaction over HZSM-5 catalysts has been clearly identified as autocatalysis mechanism, with mobile olefins and aromatic products in the zeolite pore acting as competing co-catalysts. Accordingly, two distinct reaction pathways, aromatics-based and olefin-based, are active for the production of ethene and propene from methanol over HZSM-5 under reaction conditions relevant to practical operations. The aromatics-based cycle starts with toluene as the lowest sufficiently active species, while a complete olefin methylation/cracking cycle begins its turnover with propene as the lowest sufficiently active species. The aromatics-based cycle produces ethene and propene with equal carbon based selectivities, while the olefin-based cycle favors  $C_{3+}$  olefins over ethene.

The co-existence of olefins and aromatics species in the zeolite pores leads to a competition between the two cycles for chemisorbed methanol. Therefore, total activity depends on the local activities of specific hydrocarbon species and methanol conversion. Co-processing of intermediates in each catalytic cycle of the same concentrations results in identical involvements in the turnover and in turn an identical impact on the product distribution, due to the comparable rate coefficients in each step of a cycle. While co-feeding lower substituted benzenes propagate the aromatics-based cycle, the olefins produced by the aromatics based cycle will subsequently propagate also the olefin based cycle. In turn, olefin



\* The included structure is used to indicate the first cyclic molecule as a hetero-atom aromatic species.

**Scheme 5.** Proposed mechanistic pathways for the formation of formaldehyde via hydrogen transfer and its involvement in deactivation and olefin formation.

homologation/cracking reactions are more important than the aromatics based cycle at higher methanol conversions, contributing to C<sub>3+</sub> higher olefin formation irrespective of the aromatics or olefinic nature of co-feeds. On the other hand, the aromatics based and the olefin based cycle operate for ethene formation, and the dominant pathway for ethene formation depends to a large extent on the reaction conditions. With an aromatics-enriched feed and/or at low reaction temperatures, the aromatics based cycle contributed predominantly, while the olefin based cycle contributes significantly as well when a high reaction temperature is adopted (such as in the MT(O)P process).

The results shown here also demonstrate the presence of a specific hydrogen transfer pathway involving chemisorbed methanol intermediates, which is significantly faster than classic hydride transfer between two olefinic species and has significant consequences for catalyst lifetime under MTO process conditions.

### Acknowledgments

The authors acknowledge the financial support from Clariant Produkte (Deutschland) GmbH and fruitful discussions within the framework of MuniCat. X.S. is thankful to Anmin Zheng for helpful discussions.

### References

- [1] C.D. Chang, *Catal. Rev. Sci. Eng.* 25 (1983) 1.
- [2] M. Stöcker, *Microporous Mesoporous Mater.* 29 (1999) 3.
- [3] T. Mokrani, M. Scurrill, *Catal. Rev. Sci. Eng.* 51 (2009) 1.
- [4] G.A. Olah, *Angew. Chem., Int. Ed.* 44 (2005) 2636.
- [5] U. Olsbye, S. Svella, M. Bjørgen, P. Beato, T.V.W. Janssens, F. Joensen, S. Bordiga, K.P. Lillerud, *Angew. Chem., Int. Ed.* 51 (2012) 5810.
- [6] S. Ilias, A. Bhan, *ACS Catal.* 3 (2013) 18.
- [7] J.F. Haw, W. Song, D.M. Marcus, J.B. Nicholas, *Acc. Chem. Res.* 36 (2003) 317.
- [8] D. Lesthaeghe, V. Van Speybroeck, G.B. Marin, M. Waroquier, *Angew. Chem., Int. Ed.* 118 (2006) 1746.
- [9] D. Lesthaeghe, V. Van Speybroeck, G.B. Marin, Waroquier, *Ind. Eng. Chem. Res.* 46 (2007) 8832.
- [10] W. Song, D.M. Marcus, H. Fu, J.O. Ehresmann, J.F. Haw, *J. Am. Chem. Soc.* 124 (2002) 3844.
- [11] N.Y. Chen, W.J. Reagan, *J. Catal.* 59 (1979) 123.
- [12] R.M. Dessau, *J. Catal.* 99 (1986) 111.
- [13] R.M. Dessau, R.B. LaPierre, *J. Catal.* 78 (1982) 136.
- [14] B.E. Langner, *Appl. Catal.* 2 (1982) 289.
- [15] T. Mole, J. Whiteside, D. Seddon, *J. Catal.* 82 (1983) 261.
- [16] T. Mole, G. Bett, D. Seddon, *J. Catal.* 84 (1983) 435.
- [17] I.M. Dahl, S. Kolboe, *Catal. Lett.* 20 (1993) 329.
- [18] I.M. Dahl, S. Kolboe, *J. Catal.* 149 (1994) 458.
- [19] I.M. Dahl, S. Kolboe, *J. Catal.* 161 (1996) 304.
- [20] J.F. Haw, J.B. Nicholas, W. Song, F. Deng, Z. Wang, T. Xu, C.S. Heneghan, *J. Am. Chem. Soc.* 122 (2000) 4763.
- [21] Ø. Mikkelsen, P.O. Rønning, S. Kolboe, *Microporous Mesoporous Mater.* 40 (2000) 95.
- [22] B. Arstad, S. Kolboe, *Catal. Lett.* 71 (2001) 209.
- [23] B. Arstad, S. Kolboe, *J. Am. Chem. Soc.* 123 (2001) 8137.
- [24] W. Song, J.F. Haw, J.B. Nicholas, C.S. Henghan, *J. Am. Chem. Soc.* 122 (2000) 10726.
- [25] W. Song, H. Fu, J.F. Haw, *J. Am. Chem. Soc.* 123 (2001) 4749.
- [26] W. Song, H. Fu, J.F. Haw, *J. Phys. Chem. B* 105 (2001) 12839.
- [27] W. Song, H. Fu, J.F. Haw, *Catal. Lett.* 76 (2001) 89.
- [28] J.F. Haw, D.M. Marcus, *Catal. Lett.* 34 (2005) 41.
- [29] M. Bjørgen, U. Olsbye, S. Kolboe, *J. Catal.* 215 (2003) 30.
- [30] M. Bjørgen, U. Olsbye, D. Petersen, S. Kolboe, *J. Catal.* 221 (2004) 1.
- [31] D. Lesthaeghe, J. Van der Mynsbrugge, M. Vandichel, M. Waroquier, V. Van Speybroeck, *ChemCatChem* 3 (2011) 208.
- [32] S. Teketel, S. Svella, K.P. Lillerud, U. Olsbye, *ChemCatChem* 1 (2009) 78.
- [33] S. Teketel, U. Olsbye, K.P. Lillerud, P. Beato, S. Svella, *Microporous Mesoporous Mater.* 136 (2010) 33.
- [34] J. Li, Y. Wei, Y. Qi, P. Tian, B. Li, Y. He, F. Chang, X. Sun, Z. Liu, *Catal. Today* 164 (2011) 288.
- [35] J.H. Ahn, B. Temel, E. Iglesia, *Angew. Chem., Int. Ed.* 121 (2009) 3872.
- [36] D.A. Simonetti, J.H. Ahn, E. Iglesia, *J. Catal.* 277 (2011) 173.
- [37] S. Svella, F. Joensen, J. Nerlov, U. Olsbye, K.P. Lillerud, S. Kolboe, M. Bjørgen, *J. Am. Chem. Soc.* 126 (2006) 14770.
- [38] M. Bjørgen, S. Svella, F. Joensen, J. Nerlov, S. Kolboe, F. Bonino, L. Palumbo, S. Bordiga, U. Olsbye, *J. Catal.* 248 (2007) 195.
- [39] H. Koempel, W. Liebner, *Stud. Surf. Sci. Catal.* 167 (2007) 261.
- [40] H. Bach, L. Brehm, S. Jensen, *EP 2004/018089 A1*, 2004.
- [41] G. Birke, H. Koempel, W. Liebner, H. Bach, *EP2006048184*, 2006.
- [42] M. Rothaemel, U. Finck, T. Renner, *EP 2006/136433 A1*, 2006.
- [43] X. Sun, S. Mueller, H. Shi, G.L. Haller, M. Sanchez-Sanchez, A.C. van Veen, J.A. Lercher, *J. Catal.* 314 (2014) 21.
- [44] S. Svella, P.O. Rønning, U. Olsbye, S. Kolboe, *J. Catal.* 224 (2005) 385.
- [45] S. Svella, P.O. Rønning, S. Kolboe, *J. Catal.* 224 (2004) 115.
- [46] I.M. Hill, Y.S. Ng, A. Bhan, *ACS Catal.* 2 (2012) 1742.
- [47] I.M. Hill, S.A. Hashimi, A. Bhan, *J. Catal.* 291 (2012) 155.
- [48] I.M. Hill, S.A. Hashimi, A. Bhan, *J. Catal.* 285 (2012) 115.
- [49] G. Mirth, J.A. Lercher, *J. Phys. Chem.* 95 (1991) 3736.
- [50] J. Van der Mynsbrugge, M. Visur, U. Olsbye, P. Beato, M. Bjørgen, V. Van Speybroeck, S. Svella, *J. Catal.* 29 (2012) 201.
- [51] M. Bjørgen, F. Joensen, K.P. Lillerud, U. Olsbye, S. Svella, *Catal. Today* 142 (2009) 90.
- [52] W.O. Haag, R.M. Lago, P.G.J. Rodewald, *Mol. Catal.* 17 (1982) 161.
- [53] W. Wu, W. Guo, W. Xiao, M. Luo, *Chem. Eng. Sci.* 66 (2011) 4722.
- [54] U.V. Mentzel, S. Shunmugavel, S.L. Hruby, C.H. Christensen, M.S. Holm, *J. Am. Chem. Soc.* 131 (2009) 17009.
- [55] G.F. Hutchings, F. Gottschalk, R. Hunter, *Ind. Eng. Chem. Res.* 26 (1987) 637.